

CONFIRMATION OF THE REMARKABLE COMPACTNESS OF MASSIVE QUIESCENT GALAXIES AT $z \sim 2.3$: EARLY-TYPE GALAXIES DID NOT FORM IN A SIMPLE MONOLITHIC COLLAPSE^{1,2}

PIETER G. VAN DOKKUM,³ MARIJN FRANX,⁴ MARISKA KRIEK,⁵ BRADFORD HOLDEN,⁶ GARTH D. ILLINGWORTH,⁶
DANIEL MAGEE,⁶ RYCHARD BOUWENS,⁶ DANILO MARCHESINI,³ RYAN QUADRI,⁴
GREG RUDNICK,⁷ EDWARD N. TAYLOR,⁴ AND SUNE TOFT⁸

Received 2008 February 8; accepted 2008 February 27; published 2008 March 19

ABSTRACT

Using deep near-infrared spectroscopy, Kriek et al. found that $\sim 45\%$ of massive galaxies at $z \sim 2.3$ have evolved stellar populations and little or no ongoing star formation. Here we determine the sizes of these quiescent galaxies using deep, high-resolution images obtained with *HST*/NIC2 and laser guide star (LGS)-assisted Keck/adaptive optics (AO). Considering that their median stellar mass is $1.7 \times 10^{11} M_{\odot}$, the galaxies are remarkably small, with a median effective radius $r_e = 0.9$ kpc. Galaxies of similar mass in the nearby universe have sizes of ≈ 5 kpc and average stellar densities that are 2 orders of magnitude lower than the $z \sim 2.3$ galaxies. These results extend earlier work at $z \sim 1.5$ and confirm previous studies at $z > 2$ that lacked spectroscopic redshifts and imaging of sufficient resolution to resolve the galaxies. Our findings demonstrate that fully assembled early-type galaxies make up at most $\sim 10\%$ of the population of K -selected quiescent galaxies at $z \sim 2.3$, effectively ruling out simple monolithic models for their formation. The galaxies must evolve significantly after $z \sim 2.3$, through dry mergers or other processes, consistent with predictions from hierarchical models.

Subject headings: cosmology: observations — galaxies: evolution — galaxies: formation

1. INTRODUCTION

The sizes of massive galaxies at high redshift provide strong constraints on galaxy formation models. Models starting from Λ CDM initial conditions have predicted that the progenitors of today's early-type galaxies should be smaller by a factor of a few at redshifts of 2–3 (e.g., Loeb & Peebles 2003; Robertson et al. 2006; Khochfar & Silk 2006; Naab et al. 2007). This can be contrasted to expectations from simple “monolithic” models (e.g., Eggen et al. 1962), in which galaxies undergo little or no structural evolution since their initial assembly at very high redshift.

Several recent studies have found evidence that massive galaxies at high redshift are indeed quite compact, particularly those with the lowest estimated star formation rates (Daddi et al. 2005; Trujillo et al. 2006, 2007; Zirm et al. 2007; Toft et al. 2007; Longhetti et al. 2007; Cimatti et al. 2008). The size evolution appears to be quite dramatic; Toft et al. (2007) find that, on average, the quiescent $z \sim 2.5$ galaxies in their sample have a factor of 30–40 higher surface density than do red galaxies of the same mass in the Sloan Digital Sky Survey (SDSS).

These results are still somewhat tentative, due to various systematic uncertainties. First, the galaxies were selected in relatively small fields and, therefore, typically do not span the mass range of today's giant elliptical galaxies ($M \gtrsim 10^{11} M_{\odot}$). Second, the imaging that has been used so far has either sam-

pled the rest-frame ultraviolet (e.g., Cimatti et al. 2008) or not been of sufficient resolution to measure accurate rest-frame optical sizes of very compact objects. Third, some of the galaxies may have a central starburst or active nucleus that could skew their size measurements. Fourth, the stellar ages and masses of the galaxies have large uncertainties, as their broadband photometry can typically be fitted by a wide range of models (see, e.g., Papovich et al. 2001). Lastly, and perhaps most importantly, studies at $z > 2$ are typically based on photometric redshifts, which are poorly calibrated for faint, red galaxies.

Recently, Kriek et al. (2006) used extensive near-infrared spectroscopy to secure the first sample of *spectroscopically confirmed* massive ($M \gtrsim 10^{11} M_{\odot}$) galaxies with evolved stellar populations at $z > 2$. In this Letter, we present high-quality *HST* NIC2 and Keck images of these galaxies to measure accurate rest-frame optical sizes. The nine objects discussed here are the oldest objects in a complete sample of K -selected massive galaxies at $z \sim 2.3$. If early-type galaxies were already fully formed at this redshift, we should see no structural differences between these galaxies and galaxies of similar mass at $z = 0$.

2. SAMPLE, OBSERVATIONS, AND REDUCTION

Kriek et al. (2006, 2008a) present a deep near-IR spectroscopic survey of K -selected galaxies at $2 < z < 2.7$ with the Gemini Near-Infrared Spectrograph (GNIRS). The galaxies were originally identified in the deep, wide Multiwavelength Survey by Yale-Chile (MUSYC; Quadri et al. 2007). One of the key findings of Kriek et al. is that nearly half of the galaxies show no detected $H\alpha$ emission and have spectra dominated by strong Balmer/4000 Å breaks. Nine of these quiescent objects were presented in Kriek et al. (2006). These nine galaxies have a median redshift of 2.34, stellar masses $\gtrsim 10^{11} M_{\odot}$, and ages of 0.5–1 Gyr. They define a tight red sequence in rest-frame $U - B$ (Kriek et al. 2008b).

All nine quiescent galaxies were observed in the F160W

¹ Based on observations with the NASA/ESA *Hubble Space Telescope* (*HST*), obtained at the Space Telescope Science Institute, which is operated by AURA, Inc., under NASA contract NAS 5–26555.

² Based on observations obtained with the W. M. Keck Observatory, which was made possible by the generous financial support of the W. M. Keck Foundation.

³ Department of Astronomy, Yale University, New Haven, CT 06520-8101.

⁴ Sterrewacht Leiden, Leiden University, NL-2300 RA Leiden, Netherlands.

⁵ Department of Astrophysical Sciences, Princeton University, Princeton, NJ 08544.

⁶ UCO/Lick Observatory, University of California, Santa Cruz, CA 95064.

⁷ National Optical Astronomical Observatory, Tucson, AZ 85719.

⁸ European Southern Observatory, D-85748 Garching, Germany.

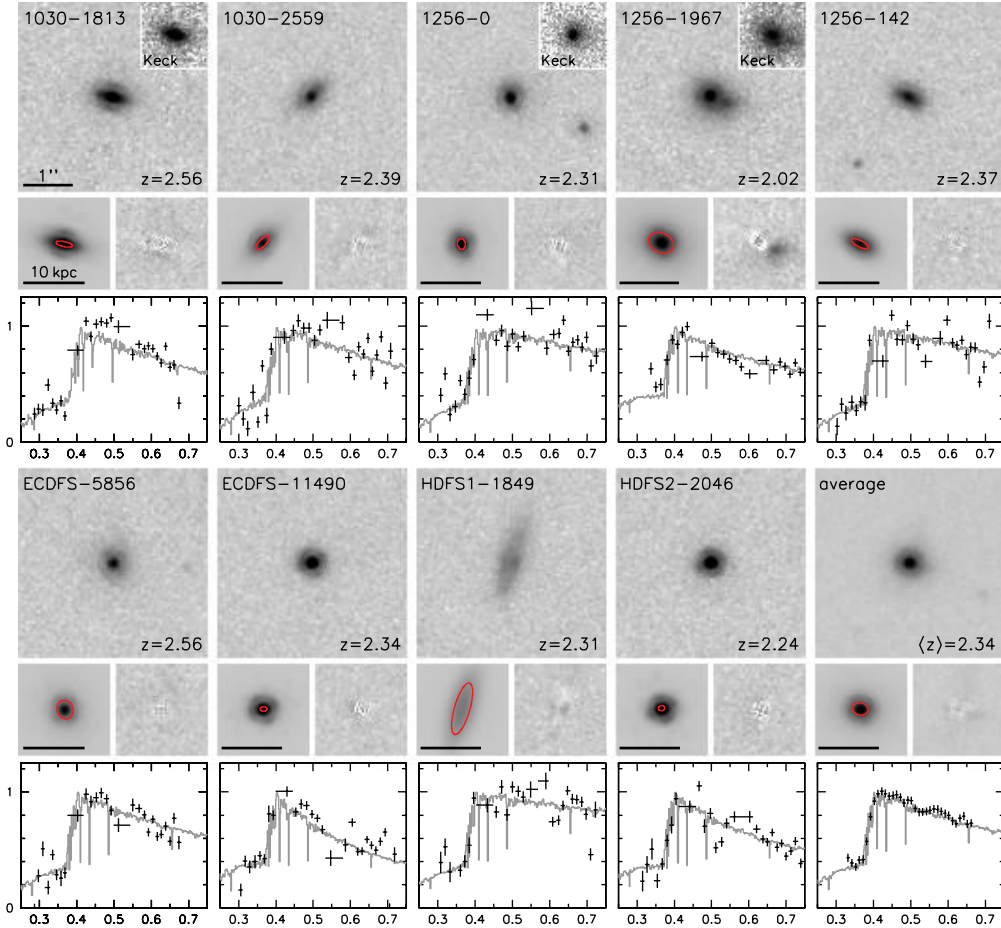


FIG. 1.—*HST* NIC2 images of the nine spectroscopically confirmed quiescent $z > 2$ galaxies from Kriek et al. (2006). Each panel spans $3.8'' \times 3.8''$; north is up, and east is to the left. The small panels below each galaxy show the best-fitting Sérsic model (convolved with the PSF) and the residual after subtraction of the best-fitting model. The red ellipses are constructed from the best-fitting effective radii, axis ratios, and position angles. Note that the ellipses are significantly smaller than 10 kpc, which is the effective diameter of typical massive elliptical galaxies in the nearby universe. Gemini GNIRS spectra from Kriek et al. (2006) are also shown. Insets show Keck LGS/AO images of three galaxies.

filter using the NIC2 camera on *HST*, from 2006 June–2007 June. Two orbits were used for each of the brightest two galaxies, and three orbits for each of the remaining seven. Each orbit was split in two (dithered) exposures. The reduction followed the procedures outlined in Bouwens & Illingworth (2006) and R. Bouwens et al., in preparation. Before combining, we drizzled the individual exposures to a new grid with $0.0378''$ pixels to ensure that the point-spread function (PSF) is well sampled. Images of the nine galaxies are shown in Figure 1.

TABLE 1
STRUCTURAL PARAMETERS

ID	z	r_e^a (kpc)	\pm	n	\pm	b/a	\pm
1030-1813	2.56	0.76	0.06	1.9	0.5	0.30	0.03
1030-2559	2.39	0.92	0.18	2.3	0.6	0.39	0.04
1256-0	2.31	0.78	0.17	3.2	0.9	0.71	0.10
1256-1967	2.02	1.89	0.15	3.4	0.1	0.75	0.07
1256-142	2.37	0.93	0.04	0.9	0.3	0.35	0.04
ECDFS-5856	2.56	1.42	0.35	4.5	0.4	0.83	0.07
ECDFS-11490	2.34	0.47	0.03	2.8	0.8	0.63	0.07
HDFS1-1849	2.31	2.38	0.11	0.5	0.2	0.29	0.02
HDFS2-2046	2.24	0.49	0.02	2.3	0.8	0.76	0.08

^a Circularized effective radius.

Three of the galaxies (1030-1813, 1256-0, and 1256-1967) were also observed with Keck, using LSG AO to correct for the atmosphere. The data were obtained on 2007 May 14 and 2008 January 13 using the NIRC2 wide-field camera, which gives a pixel size of $0.04''$. The reduction followed standard procedures for near-IR imaging data. The Keck images are shown as insets in Figure 1. They show the same qualitative features as the NICMOS data.

3. FITTING

Each galaxy was fitted with a Sérsic (1968) radial surface brightness profile, using the two-dimensional fitting code GALFIT (Peng et al. 2002). The Sérsic n -parameter allows for a large range of profile shapes and provides a crude estimate of the bulge-to-disk ratio. For each galaxy, a synthetic NIC2 PSF was created by generating subsampled PSFs with Tiny Tim 6.3 (Krist 1995), shifting them to replicate the location of the galaxy on the individual exposures, binning these to the native NIC2 resolution, and finally drizzling these “observations” to the grid of the galaxy images. The resulting fit parameters are listed in Table 1; ellipses corresponding to the best-fit parameters are indicated in red in Figure 1. The (circularized) effective radii were transformed to kiloparsecs using $H_0 = 70 \text{ km s}^{-1} \text{ Mpc}^{-1}$, $\Omega_m = 0.3$, and $\Omega_\Lambda = 0.7$.

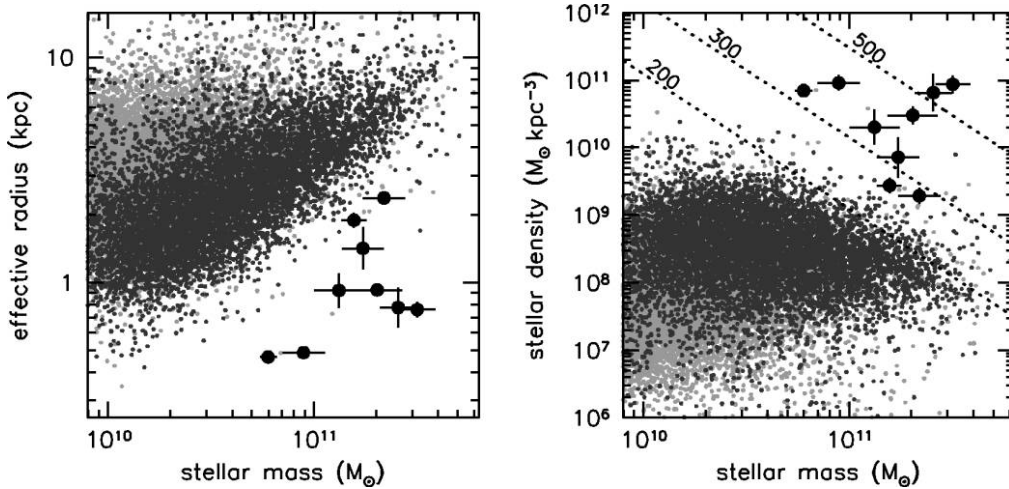


FIG. 2.—Relations between size and (total) stellar mass (*left panel*) and between the average stellar density inside the effective radius and stellar mass (*right panel*). Large symbols with error bars are the quiescent $z \sim 2.3$ galaxies. Small symbols are SDSS galaxies, with galaxies that are not on the red sequence in light gray. The dotted lines indicate the expected location of galaxies with stellar velocity dispersions of 200, 300, and 500 km s^{-1} . The high-redshift galaxies are much smaller and denser than SDSS galaxies of the same stellar mass.

Uncertainties in the structural parameters of faint galaxies are difficult to estimate, as they are usually dominated by systematic effects. For each galaxy, we added the residual image of each of the other galaxies (excluding 1256-1967) in turn, repeated the fit, and determined the rms of the seven values obtained from these fits. The uncertainties listed in Table 1 are $2 \times$ these rms values, to account for additional systematic uncertainties. These were assessed by changing the size of the fitting region, scrambling the subpixel positions of the galaxies, and changing the drizzle grid.

The Keck images offer an independent test of the reliability of the fit parameters. Fitting the Keck images with a range of stellar PSFs (including stars in the field of view) gives results that are consistent with the NIC2 fits within the listed uncertainties. As an example, for 1030-1813, we find $r_e = 0.73$ kpc, $n = 1.6$, and $b/a = 0.32$ from the Keck image. In the following, we will use the values derived from the higher signal-to-noise ratio (S/N) NIC2 images; our conclusions would not change if we were to use the Keck results for 1030-1813, 1256-0, and 1256-1967.

4. SIZES AND DENSITIES

The most remarkable aspect of the $z \sim 2.3$ galaxies is their compactness. The circularized effective radii range from 0.5 to 2.4 kpc, and the median is 0.9 kpc. To put this in context, this is smaller than many bulges of spiral galaxies (including the bulges of the Milky Way and M31, which have $r_e \approx 2.5$ kpc; van den Bergh 1999). In the left panel of Figure 2, the sizes are compared to those of SDSS galaxies. The SDSS data were taken from the New York University Value-Added Galaxy Catalog (Blanton et al. 2005) in a narrow redshift range, with various small corrections (M. Franx et al., in preparation). Dark gray points are galaxies on the red sequence, here defined as $u - g = 0.1 \log M + (0.6 \pm 0.2)$. Stellar masses for the $z \sim 2.3$ galaxies were taken from Kriek et al. (2008a) and corrected to a Kroupa (2001) initial mass function (IMF). The median mass of the $z \sim 2.3$ galaxies is $1.7 \times 10^{11} M_\odot$. The median r_e of SDSS red sequence galaxies with masses $(1.5\text{--}1.9) \times 10^{11} M_\odot$ is 5.0 kpc, a factor of ~ 6 larger than the median size of the $z \sim 2.3$ galaxies.

The combination of small sizes and high masses implies very

high densities. The right panel of Figure 2 shows the relation between stellar density and stellar mass, with density defined as $\rho = 0.5M/[(4/3)\pi r_e^3]$ (i.e., the mean stellar density within the effective radius, assuming a constant stellar mass-to-light $[M/L]$ ratio with radius). The median density of the $z \sim 2.3$ galaxies is $3 \times 10^{10} M_\odot \text{ kpc}^{-3}$ (with a considerable rms scatter of 0.7 dex), a factor of ~ 180 higher than the densities of local red sequence galaxies of the same mass.

We note that it is difficult to determine the morphologies of the galaxies, as they are so small. Nevertheless, it is striking that several galaxies are quite elongated (see Fig. 1). The most elongated galaxies are also the ones with the lowest n -values (the correlation between n and b/a is formally significant at the $>99\%$ level⁹), and a possible interpretation is that the light of a subset of the galaxies is dominated by very compact, massive disks (see § 5).

5. DISCUSSION

We find that all ($100^{+0}_{-1}\%$) of the quiescent, massive galaxies at $\langle z \rangle = 2.3$ spectroscopically identified by Kriek et al. (2006) are extremely compact, having a median effective radius of only 0.9 kpc. This result extends previous work at $z \sim 1.5$ (Trujillo et al. 2007; Longhetti et al. 2007; Cimatti et al. 2008) and confirms other studies at similar redshifts that were based on photometric redshifts and images of poorer quality (Zirm et al. 2007; Toft et al. 2007). Our study, together with the spectroscopy in Kriek et al. (2006) demonstrating that the H -band light comes from evolved stars, shows that the small measured sizes of evolved high-redshift galaxies are not caused by photometric redshift errors, active galactic nuclei, dusty starbursts, or measurement errors.

It is remarkable that all nine galaxies are so compact; even the largest galaxy in the sample (HDFS1-1849) is significantly offset from the relations of red galaxies in the nearby universe (see Fig. 2). We do not find any galaxy resembling a fully assembled elliptical or S0 galaxy, which means that such objects make up less than $\sim 10\%$ of the population of quiescent galaxies at $z \sim 2.3$. This result effectively rules out simple

⁹ There is no significant correlation between r_e and n , or between r_e and b/a .

monolithic models, in which early-type galaxies are assembled at the same time as their stars, and is arguably the most direct evidence to date for an essentially hierarchical assembly history for massive galaxies.

Our results are qualitatively consistent with recent hydrodynamical simulations in a Λ CDM universe, which predict that the stars in the central parts of massive elliptical galaxies formed rapidly at $z \sim 5$ out of a concentrated gas distribution (e.g., Naab et al. 2007). Observationally, it is tempting to link the compact $z \sim 2.3$ galaxies to the rapidly rotating, dense molecular gas reservoirs associated with some submillimeter galaxies¹⁰ (Tacconi et al. 2008) and high-redshift quasars (e.g., Riechers et al. 2006; Narayanan et al. 2008). The fact that several of the galaxies in our sample (and the two galaxies identified by Stockton et al. 2008) appear to be disks provides indirect support for this idea.

Various mechanisms can play a role in bringing the $z \sim 2.3$ galaxies onto the scaling relations followed by today's red galaxies. The total mass in galaxies on the red sequence increases by a factor of ~ 8 from $z \sim 2.3$ to $z = 0$ (Kriek et al. 2008b), and the galaxies that are added after $z \sim 2.3$ may have preferentially larger sizes than the galaxies that are already in place at that redshift. We note, however, that the galaxies described here are quite extreme, even when compared to the most compact 10% of today's massive galaxies. Furthermore, mass loss from stellar winds will decrease the stellar mass (and increase the radius) from $z = 2.3$ to $z = 0$. Finally, accretion of satellites (e.g., Naab et al. 2007) and dry mergers (e.g., van Dokkum 2005) may increase the sizes over time. Mergers will, to first order, move galaxies roughly parallel to the size-mass relation, but the effects on the sizes may be stronger in simulations with realistic boundary conditions (see Naab et al. 2007). Also, the smallest galaxies are likely to merge with larger galaxies, and even a merger between two small galaxies will (obviously) reduce their number. Each of these mechanisms could plausibly alter the size-mass relation by a factor of 1.5–2 but not a factor of ~ 6 . This means that some combination of effects is required to bring the compact $z \sim 2.3$ galaxies to the local relations or that we have not yet identified the main mechanism.

We also cannot exclude the possibility that we are overes-

¹⁰ Note, however, that these submillimeter galaxies would have to be at significantly higher redshift than the objects discussed in Tacconi et al. (2008).

timating the densities of these galaxies, as there are several systematic uncertainties in the analysis. First, we may be underestimating the sizes of the objects if their morphologies are complex. In particular, an extended low surface brightness component could be “hiding” in the noise, in which case the measured effective radius would be larger if we had data of higher S/N. There is no evidence for this from fitting a Sérsic profile to the stacked image of the nine galaxies (see Fig. 1), but we do note that the galaxies are on average ~ 0.2 mag brighter in ground-based images (which include any extended emission) than in the *HST* images. A more subtle effect is an age-induced radial gradient in the M/L ratio of the galaxies, such that the central parts are younger than the outer parts. If this is the case, the mass-weighted r_e could be significantly larger than the luminosity-weighted r_e . Such a spatial arrangement arises in several different classes of models for the formation of massive ellipticals (Robertson et al. 2006; Naab et al. 2007; P. Hopkins et al., in preparation). Lastly, the IMF might be weighted toward high-mass stars in these systems. Several studies have argued that the IMF in the progenitors of elliptical galaxies may have been deficient in low-mass stars, which would impact their inferred masses and densities (e.g., Larson 2005; van Dokkum 2008). The precise effect depends on the assumed form of the IMF and can be a factor of ~ 2 for plausible parameters (see van Dokkum 2008).

There are several ways to improve on the results presented here. Radial gradients in the M/L ratio can, in principle, be measured from high-quality imaging in multiple passbands. Very deep imaging can provide better constraints on the surface brightness profiles at large radii. Ultimately, kinematics should provide the most direct information on the nature of these compact objects (see also Toft et al. 2007 and Cimatti et al. 2008). As shown by the dotted lines in Figure 2 (derived from the relation between M , σ , and r_e given in van Dokkum & Stanford 2003), the implied velocities are very high at 300–500 km s⁻¹. Finally, it will be interesting to build up spectroscopic samples that are fainter in K , as this will allow us to extend the analysis to lower masses and to determine the sizes of quiescent massive galaxies with higher M/L ratios than the objects studied here.

We thank the referee, Ulrich Hopp, for his comments. Support from NASA grant HST-GO-10808.01-A is gratefully acknowledged.

REFERENCES

- Blanton, M. R., et al. 2005, *AJ*, 129, 2562
 Bouwens, R. J., & Illingworth, G. D. 2006, *Nature*, 443, 189
 Cimatti, A., et al. 2008, *A&A*, in press (astro-ph/0801.1184)
 Daddi, E., et al. 2005, *ApJ*, 626, 680
 Eggen, O. J., Lynden-Bell, D., & Sandage, A. R. 1962, *ApJ*, 136, 748
 Khochfar, S., & Silk, J. 2006, *ApJ*, 648, L21
 Kriek, M., et al. 2006, *ApJ*, 649, L71
 ———. 2008a, *ApJ*, in press (astro-ph/0801.1110)
 ———. 2008b, *ApJ*, submitted
 Krist, J. 1995, in *ASP Conf. Ser. 77, Astronomical Data Analysis Software and Systems IV*, ed. R. A. Shaw, H. E. Payne, & J. J. E. Hayes (San Francisco: ASP), 349
 Kroupa, P. 2001, *MNRAS*, 322, 231
 Larson, R. B. 2005, *MNRAS*, 359, 211
 Loeb, A., & Peebles, P. J. E. 2003, *ApJ*, 589, 29
 Longhetti, M., et al. 2007, *MNRAS*, 374, 614
 Naab, T., Johansson, P. H., Ostriker, J. P., & Efstathiou, G. 2007, *ApJ*, 658, 710
 Narayanan, D., et al. 2008, *ApJS*, 174, 13
 Papovich, C., Dickinson, M., & Ferguson, H. C. 2001, *ApJ*, 559, 620
 Peng, C. Y., Ho, L. C., Impey, C. D., & Rix, H.-W. 2002, *AJ*, 124, 266
 Quadri, R., et al. 2007, *AJ*, 134, 1103
 Riechers, D. A., et al. 2006, *ApJ*, 650, 604
 Robertson, B., Cox, T. J., Hernquist, L., Franx, M., Hopkins, P. F., Martini, P., & Springel, V. 2006, *ApJ*, 641, 21
 Sérsic, J. L. 1968, *Atlas de Galaxias Australes* (Cordoba: Obs. Astron.)
 Stockton, A., McGrath, E., Canalizo, G., Iye, M., & Maihara, T. 2008, *ApJ*, 672, 146
 Tacconi, L. J., et al. 2008, *ApJ*, in press (astro-ph/0801.3650)
 Toft, S., et al. 2007, *ApJ*, 671, 285
 Trujillo, I., Conselice, C. J., Bundy, K., Cooper, M. C., Eisenhardt, P., & Ellis, R. S. 2007, *MNRAS*, 382, 109
 Trujillo, I., et al. 2006, *ApJ*, 650, 18
 van den Bergh, S. 1999, *A&A Rev.*, 9, 273
 van Dokkum, P. G. 2005, *AJ*, 130, 2647
 ———. 2008, *ApJ*, 674, 29
 van Dokkum, P. G., & Stanford, S. A. 2003, *ApJ*, 585, 78
 Zirm, A. W., et al. 2007, *ApJ*, 656, 66